life

MDPI

Article

Post-Weaning Antibiotic-Induced Dysbiosis Is Associated with Alterations in Growth and Nucleobindin-2/Nesfatin-1-Related Outcomes in Rats

Gokcen Guvenc-Bayram [1,*], Songul Fidan-Bulut [2], Gozde Arslan [3], Fatmanur Dundar [3], Duygu Gok-Yurtseven [4], Gonca Topal [4], Zeynep Semen [5,6], Duygu Udum [7] and Murat Yalcin [2]

1 Department of Physiology, Faculty of Veterinary Medicine, Dokuz Eylul University, 35390 Izmir, Türkiye
2 Department of Physiology, Faculty of Veterinary Medicine, Bursa Uludag University, 16059 Bursa, Türkiye; fidansongul54@gmail.com (S.F.-B.); muraty@uludag.edu.tr (M.Y.)
3 Department of Immunology, Faculty of Medicine, Bursa Uludag University, 16059 Bursa, Türkiye; arslangozde9337@gmail.com (G.A.); fatmanurdn39@gmail.com (F.D.)
4 Department of Histology and Embryology, Faculty of Medicine, Bursa Uludag University, 16059 Bursa, Türkiye; dgok@uludag.edu.tr (D.G.-Y.); goncatopal.1992@gmail.com (G.T.)
5 Department of Biochemistry, Faculty of Veterinary Medicine, Dokuz Eylul University, 35390 Izmir, Türkiye; zeynep.semen@deu.edu.tr
6 Comparative Pediatrics, Section for Biomedicine, Department of Veterinary and Animal Sciences, University of Copenhagen, 1870 Frederiksberg, Denmark
7 Department of Biochemistry, Faculty of Veterinary Medicine, Bursa Uludag University, 16059 Bursa, Türkiye; cduygudum@gmail.com
* Correspondence: gokcen.guvencbayram@deu.edu.tr

Abstract

The gut microbiota interacts with host metabolic and neuroendocrine processes, and nesfatin-1, derived from nucleobindin-2 (NUCB2), regulates appetite and energy homeostasis. We investigated whether post-weaning antibiotic-induced dysbiosis (DYS) is associated with altered NUCB2/nesfatin-1 signaling, feed intake, and growth, and whether fecal microbiota transplantation (FMT) is associated with partial recovery. After weaning, 28 male Sprague-Dawley rats were assigned to control (CON, n = 8), DYS (n = 10), or FMT (n = 10) groups. DYS was induced with vancomycin and amoxicillin for 2 weeks, followed by 10 days of FMT. Body weight and feed intake were monitored weekly. Cecal microbiota were characterized descriptively by shotgun sequencing of pooled samples. Plasma and cecal nesfatin-1 were measured by ELISA, cecal NUCB2 mRNA by qPCR, and gastric nesfatin-1 immunoreactivity by immunohistochemistry. DYS was associated with markedly fewer detected microbial taxa in the pooled cecal metagenome, reduced feed intake and body weight, higher plasma nesfatin-1 concentrations, higher cecal nesfatin-1 immunoreactivity and NUCB2 mRNA expression, and lower gastric nesfatin-1 immunoreactivity. After FMT, feed intake showed an increasing trend whereas body weight did not differ significantly from DYS; the nesfatin-1 and NUCB2 mRNA measures were lower and gastric immunoreactivity was higher, without reaching control values. DYS was thus associated with altered NUCB2/nesfatin-1-related outcomes, reduced feed intake, and lower body weight gain, and FMT was associated with partial attenuation of these changes.

Keywords: dysbiosis; fecal microbiota transplantation; nucleobindin-2; nesfatin-1; feed intake; growth

Check for updates

Academic Editor: Qi-Ye Wang

Received: 20 October 2026
Revised: 12 November 2026
Accepted: 16 November 2026
Published: 18 November 2026

Copyright: © 2026 by the authors. Licensee MDPI, Basel, Switzerland. This article is an open access article distributed under the terms and conditions of the Creative Commons Attribution (CC BY) license.

1. Introduction

The gut microbiota plays a fundamental role in host metabolism, energy homeostasis, and neuroendocrine regulation [1]. Increasing evidence suggests that perturbations of gut microbial communities, known as dysbiosis (DYS), are associated with metabolic disturbances, obesity, inflammatory disorders, and impaired neuroendocrine signaling [2,3]. A major mechanistic link underlying these associations is the gut–brain axis, a bidirectional communication network in which microbial metabolites, immune mediators, and neural pathways influence appetite, mood, and energy balance [1,4]. Understanding this crosstalk is crucial for elucidating how intestinal DYS affects systemic metabolic regulation.

Among the neuropeptides involved in appetite and energy control, nesfatin-1, derived from the nucleobindin-2 (NUCB2) precursor protein, has gained increasing attention. Nesfatin-1 is widely expressed in the hypothalamus, stomach, and intestinal tissues and exerts anorexigenic effects primarily through melanocortin signaling, independently of leptin signaling [5,6]. In addition to its central actions, nesfatin-1 acts peripherally, contributing to glucose and lipid metabolism, and gastrointestinal motility [7,8]. Despite its diverse roles, whether and how alterations in the gut microbiota influence NUCB2/nesfatin-1 expression and signaling remains largely unclear.

Broad-spectrum antibiotics are widely used to induce experimental DYS and to probe the physiological consequences of disrupting the gut microbiota. Such interventions have been shown to affect nutrient absorption, growth rate, and metabolic hormone levels in rodents [9]. Conversely, fecal microbiota transplantation (FMT) has emerged as a promising approach to restore microbial balance, with beneficial outcomes in several metabolic and inflammatory conditions [10,11]. The post-weaning period is characterized by rapid growth and ongoing maturation of the gut microbiota, which may make the host particularly sensitive to microbial perturbation. However, it remains unclear whether post-weaning DYS induces changes in gastrointestinal neuropeptide systems, particularly the NUCB2/nesfatin-1 axis.

We hypothesized that post-weaning antibiotic-induced DYS would alter gut microbial ecology and modulate the NUCB2/nesfatin-1 signaling axis, thereby contributing to changes in feed intake and growth. We further hypothesized that FMT would be associated with partial attenuation of these DYS-associated alterations. In this context, this study aimed to investigate the association between alterations in the gut microbial environment and the NUCB2/nesfatin-1 signaling system during the post-weaning period by measuring nesfatin-1 concentrations in plasma and cecal contents, cecal NUCB2 mRNA expression, and gastric nesfatin-1 immunoreactivity, together with feed intake and growth. Thus, we aimed to gain initial insight into the potential involvement of gut-associated NUCB2/nesfatin-1 signaling in metabolic and neuroendocrine regulation.

2. Materials and Methods

2.1. Animals and Experimental Procedure

Nine time-mated, 2–3-month-old, pathogen-free pregnant Sprague-Dawley rats were obtained from the Bursa Uludag University Animal Breeding Center and maintained under specific-pathogen-free conditions (20–24 °C, 12-h light/dark cycle) with ad libitum access to standard chow (Supplementary Table S1) and water.

Following weaning at 4 weeks of age, 28 male pups were allocated to three groups: control (CON, n = 8; two cages), DYS (n = 10; two cages), and FMT (n = 10; two cages). Offspring from the nine dams were equally distributed among the three experimental groups, and group allocation was balanced according to body weight. No formal sample-size calculation was performed; group sizes were determined by animal availability. Animals

were housed in groups of four or five per cage as two cages per group with free access to food (Supplementary Table S1) and water.

To induce intestinal DYS, rats in the DYS and FMT groups received vancomycin (8 mg/kg/day) and amoxicillin (60 mg/kg/day) in drinking water at concentrations of 0.08 mg/mL and 0.6 mg/mL, respectively, for 2 weeks after weaning (weeks 4–6), following a previously described protocol with modifications [9]. CON rats received antibiotic-free water. For FMT, fresh fecal pellets collected from CON rats were suspended in sterile saline (100 mg/mL). Beginning 24 h after antibiotic cessation, FMT rats received 1 mL of the suspension daily by oral gavage for 10 consecutive days, as previously described by Chen et al. [11]. DYS rats received antibiotic-free water from weeks 6 to 8.

Antibiotics were administered through drinking water shared by all animals housed within the same cage. Therefore, the cage was the experimental unit for antibiotic exposure, with two cages assigned to each experimental group (CON: 2 cages; DYS: 2 cages; FMT: 2 cages). The total number of animals was 8 in CON (4 animals per cage), 10 in DYS (5 animals per cage), and 10 in FMT (5 animals per cage). FMT was administered individually by oral gavage to each rat in the FMT group. Body weight and terminal biological outcomes were measured in individual animals; however, these observations were nested within cages and were not fully independent with respect to the shared antibiotic exposure. Accordingly, potential cage-level clustering was considered when interpreting these outcomes.

At 8 weeks of age, rats were anesthetized with sevoflurane (2–4% in 100% O_2). Blood (0.5 mL) was collected by cardiac puncture into heparinized tubes and centrifuged (3000 rpm, 10 min, 4 °C), and the plasma was stored at −80 °C. Following cervical dislocation, cecal contents were harvested into sterile tubes and stored at −80 °C for metagenomic, ELISA, and qPCR analyses. Stomachs were fixed in 10% neutral-buffered formalin for histological analysis.

2.2. Metagenomic Profiling of Cecal Microbiota

Equal amounts of cecal contents were collected from each animal within each experimental group and pooled to obtain a single composite sample per group for the evaluation of bacterial and archaeal composition. This pooling strategy was adopted to obtain an exploratory overview of the group-level microbial composition, allowing preliminary characterization of antibiotic-induced dysbiosis and the potential changes associated with subsequent FMT. Shotgun metagenomic sequencing was performed on an Illumina NovaSeq 6000 platform (150-bp paired-end reads) by Sapiens Genetic Diagnosis Inc. (Istanbul, Turkiye). Because only one pooled sample per group was analyzed, no statistical comparison was possible, and microbiota alterations were evaluated descriptively.

Raw reads were quality-checked with FastQC, and low-quality bases and adapter sequences were trimmed by the service provider. Taxa were identified using the provider's standard shotgun metagenomic profiling pipeline and are reported at species level and aggregated to genus level; relative abundances are expressed relative to the profiled fraction. Sequencing depth, host-read filtering, classifier and database versions, and reporting thresholds are not reported; the profiles are therefore presented as exploratory relative abundances only, and no diversity indices were calculated. Complete relative abundance data are provided in Supplementary Table S2.

2.3. Body Weight and Feed Consumption Monitoring

Body weights were recorded individually at weekly intervals from 4 to 8 weeks of age. Because antibiotic exposure was delivered through shared drinking water, animals within the same cage shared the same treatment environment. Thus, individual body-

weight measurements were nested within cages. Feed intake was determined weekly at the cage level by subtracting the residual feed from the amount provided and was normalized to the number of animals housed in each cage. Each experimental group consisted of two cages (CON: 2 cages, 4 rats/cage; DYS: 2 cages, 5 rats/cage; FMT: 2 cages, 5 rats/cage). Consequently, the independent observational units for feed intake were the two cages per group, rather than the individual animals. Feed-intake data were therefore summarized descriptively at the cage level.

2.4. Nesfatin-1 Quantification

Cecal contents were homogenized in ice-cold PBS at a ratio of 1 g to 4 mL, sonicated for 15 min, and centrifuged at 12,000 rpm for 15 min at 4 °C. The resulting supernatants were collected for ELISA analysis. Plasma samples and cecal supernatants were analyzed using a commercial rat nesfatin-1 ELISA kit (Bioassay Technology Laboratory, Shanghai, China, Cat. No: E0878Ra; detection range, 30–9000 ng/L; sensitivity, 16.23 ng/L; intra-assay CV, 3.3–5.5%; inter-assay CV, <10%), according to the manufacturer's instructions. Before analysis, plasma and cecal supernatants samples were undiluted. Absorbance was measured at 450 nm using a microplate reader. The concentrations obtained for cecal samples represent nesfatin-1 immunoreactivity in the analyzed cecal extracts. Unless otherwise specified, these values were not converted to amounts per gram of cecal content. Matrix-specific validation, including dilution-parallelism and spike-recovery experiments, was not performed for cecal extracts.

2.5. Determination of NUCB2 mRNA Expression

For NUCB2 mRNA analysis, equal amounts of cecal content collected from all animals within each experimental group were combined to generate a single composite sample per group. RNA extraction and subsequent qPCR measurements were performed using this pooled sample, with each measurement conducted in three technical replicates. These technical replicates were used to assess analytical consistency and do not represent independent biological samples.

Total RNA was extracted from pooled cecal content, obtained by combining samples from all animals within each experimental group, using the RiboEx (GeneAll Biotechnology, Seoul, South Korea, Cat. No. 301-001) and Hybrid-R (Cat. No. 305-101) kits (GeneAll, Seoul, Korea). cDNA was synthesized using the High-Capacity cDNA Synthesis Kit (A.B.T.™, Ankara, Türkiye, Cat. No: C03-01-05; 25 °C for 10 min, 37 °C for 120 min, 85 °C for 5 min). qPCR was conducted on a QuantStudio™ 5 System using 2× SYBR Green Master Mix (A.B.T.™, Cat. No: Q03-01-05). The 20-µL reactions contained 10 µL of master mix, 0.5 µL of each primer (10 µM), 3 µL of cDNA, and 6 µL of water. Cycling conditions were 95 °C for 5 min, followed by 40 cycles of 95 °C for 30 s, 60 °C for 30 s, and 72 °C for 1 min. Primer sequences were as follows: NUCB2, forward 5′-GCA CCA GTC AGT TTT TCA AGG G-3′ and reverse 5′-AAC AGT ACC GTG CTT GGA TGG-3′ (efficiency, 98.2%; $R^2 = 0.997$); GAPDH, forward 5′-GAT GGG TGT GAA CCA CGA GAA AT-3′ and reverse 5′-GAT ACG GAT ACA TTG GGG GTA GGA A-3′ (efficiency: 101.4%, $R^2 = 0.995$). Relative gene expression was calculated using the 2^−ΔΔCt method with GAPDH as the internal control. Melt-curve analysis confirmed specific single-product amplification.

2.6. Histopathological Evaluation and Immunohistochemical Localization of Nesfatin-1

Formalin-fixed stomach samples were embedded in paraffin, sectioned at 5 µm, and stained with hematoxylin and eosin (H&E) to evaluate fundic cell morphology. For immunohistochemistry, deparaffinized sections underwent antigen retrieval in citrate buffer (pH 6.0, 60 °C, 10 min), followed by endogenous peroxidase blocking with 3% H_2O_2 in

methanol (10 min). Sections were blocked with 10% normal horse serum (1 h) and incubated overnight at 4 °C with a rabbit anti-nesfatin-1 primary antibody (1:3000; H-003-22, Phoenix Pharmaceuticals/Vector, Burlingame, CA, USA). Detection was performed using a biotinylated secondary antibody (1:300; Jackson ImmunoResearch, West Grove, PA, USA; 2 h), an avidin–biotin complex (ABC Elite Kit; 1 h), and 3,3′-diaminobenzidine as the chromogen. Staining intensity was graded semi-quantitatively as negative (0), weak (1), moderate (2), or strong (3). Scoring was performed independently by two observers who were blinded to the group allocation. The mean of the two observers' scores was used. Multiple non-consecutive sections per animal and several randomly selected fields per section were evaluated at ×20 magnification, and the scores were averaged to obtain a single value per animal. Negative controls were prepared by omitting the primary antibody and showed no specific staining.

2.7. Statistical Evaluation

Data were expressed as mean ± SEM where applicable, and $p < 0.05$ was considered statistically significant. Changes in individual body weight over time were analyzed using repeated-measures two-way ANOVA, with experimental group and time as factors, followed by Tukey's multiple-comparison test.

Feed intake was measured at the cage level and normalized to the number of animals housed in each cage. As each experimental group consisted of only two cages, feed intake data were evaluated descriptively. Group-level mean values were calculated from the two cage-level measurements to describe the observed feeding patterns. No inferential statistical comparisons were performed for feed intake because the limited number of independent cage-level observations did not support reliable statistical inference.

Differences in plasma and cecal nesfatin-1 concentrations were analyzed using one-way ANOVA followed by Tukey's post hoc test, where appropriate. Gastric nesfatin-1 immunoreactivity scores were analyzed using the Kruskal–Wallis test followed by Dunn's multiple-comparison test. Potential clustering of animals within cages was considered when interpreting individual-level outcomes.

Microbiota sequencing and NUCB2 mRNA expression results obtained from pooled samples were interpreted descriptively. Technical replicates were not considered independent biological replicates; therefore, no inferential statistical comparisons were performed for these pooled datasets.

3. Results

3.1. Effects of DYS and FMT on Cecal Microbiota Composition

Taxonomic profiling of the pooled cecal samples indicated a marked reduction in the number of detected taxa after DYS induction. In the CON sample, 54 species-level (SGB) profiles belonging to 46 genera were detected (Figure 1A), compared with only two taxa in the DYS sample, GGB49841 (76.4%) and Lactobacillus (23.6%) (Figure 1B). In the FMT sample, 22 species-level profiles (21 genera) were detected (Figure 1C; Supplementary Table S2). Lactobacillus, Ligilactobacillus, and Limosilactobacillus, which were also present in CON, were detected in FMT, whereas the dominant CON taxon GGB49841 (46.1%) was not. These are descriptive observations from one pooled sample per group, and the number of detected taxa depends on sequencing depth and reporting thresholds.

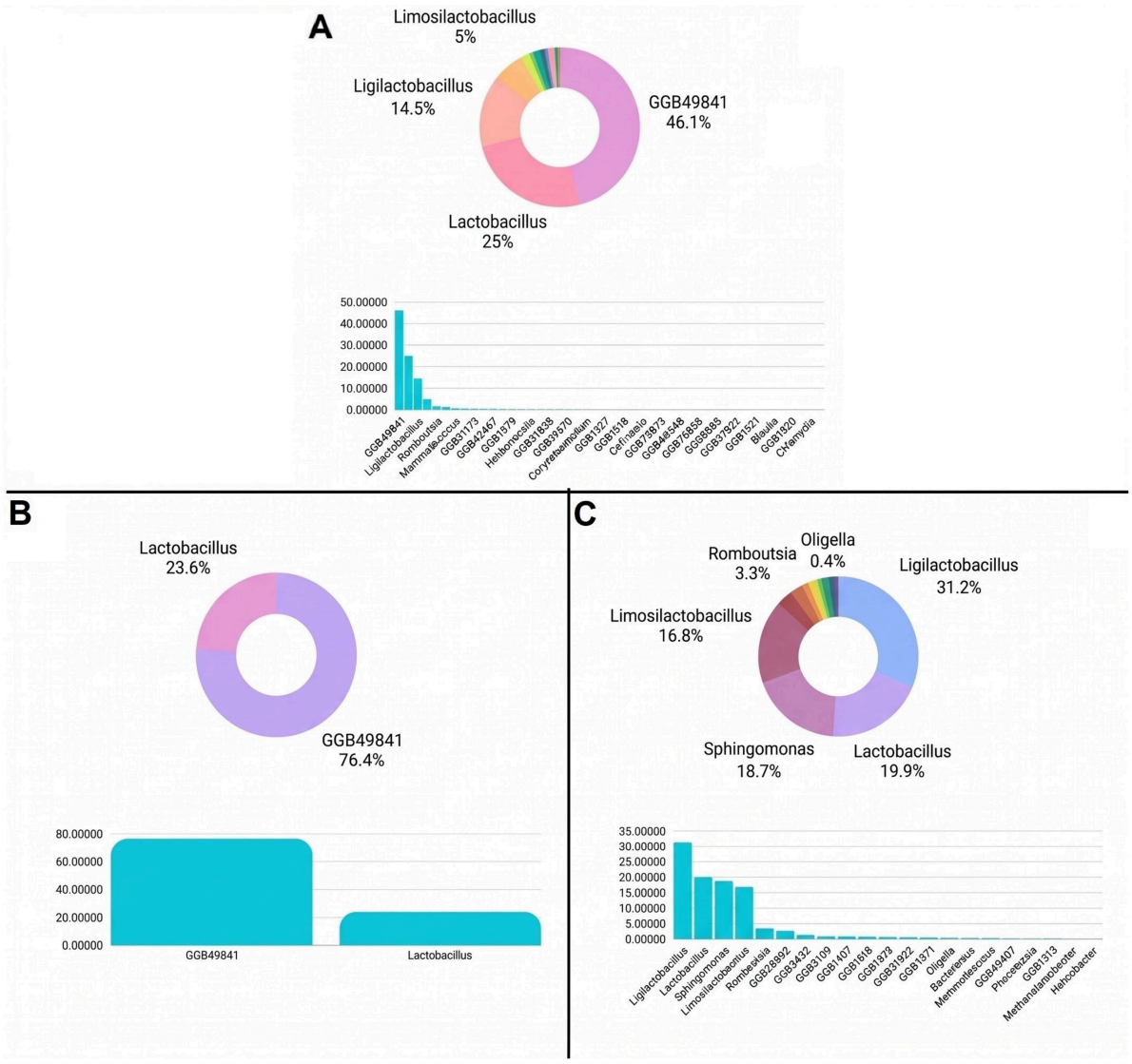


Figure 1. Genus-level distribution of the taxa identified by shotgun metagenomic sequencing in the pooled cecal samples of the CON (**A**), DYS (**B**), and FMT (**C**) groups. Relative abundances are expressed relative to the profiled fraction. One pooled sample was analyzed per group; no statistical testing was performed. Complete abundance data are provided in Supplementary Table S2.

3.2. Effects of DYS and FMT on Body Weight and Feed Consumption

At the time of group allocation following weaning (4 weeks of age), the mean body weight of the rats was approximately 73 g. Antibiotic-induced DYS was associated with a statistically significant decrease in body weight in both the DYS and FMT groups com-pared with the CON group (Figure 2A). After the initiation of FMT treatment at week 6, body weight increased gradually in the FMT group relative to the DYS group; however, this increase did not reach statistical significance (Figure 2A).

After weaning, the mean weekly feed intake per rat was approximately 102.5 g. Descriptive assessment of cage-level feed intake indicated lower consumption in the DYS and FMT groups compared with the CON group (Figure 2B). Following the initiation of FMT at the sixth week, feed intake showed an increasing trend in the FMT group relative to the DYS group (Figure 2B).

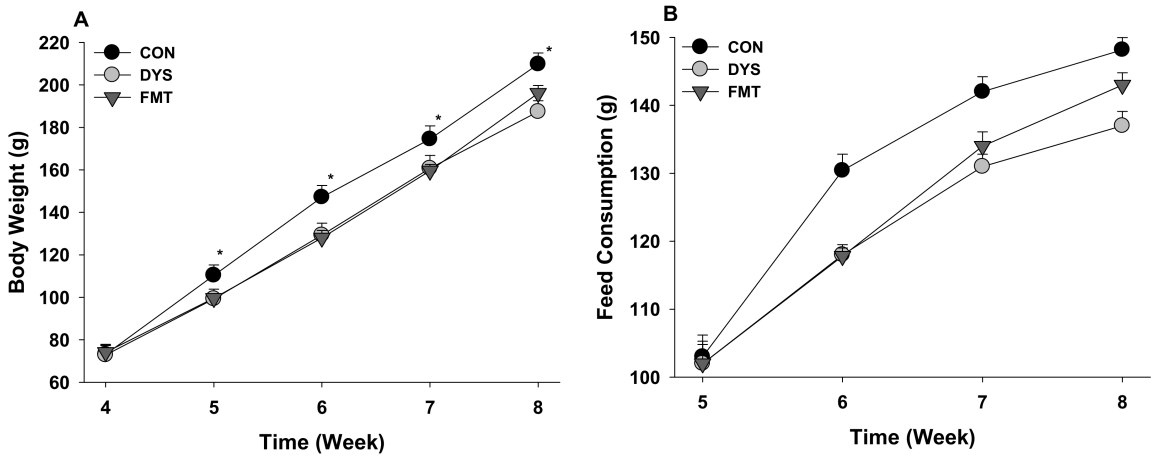


Figure 2. Body weight (**A**) and weekly feed consumption (**B**) in the CON, DYS, and FMT groups. A total of 28 male rats were included: CON (n = 8), DYS (n = 10), and FMT (n = 10). Each group consisted of two cages (CON: 4 rats/cage; DYS and FMT: 5 rats/cage). Body weight was measured individually at weekly intervals from 4 to 8 weeks of age and is presented as mean ± SEM. Statistical analysis for body weight data was performed using repeated-measures two-way ANOVA followed by Tukey's post hoc test. * $p < 0.05$ indicates a significant difference between the CON group and both the DYS and FMT groups. Feed intake was measured at the cage level, normalized per animal, and is presented descriptively based on the two cage-level observations per group. No inferential statistical testing was performed for feed intake.

3.3. Effects of DYS and FMT on Plasma and Cecal Nesfatin-1 Levels and Cecal NUCB2 mRNA Expression

Plasma nesfatin-1 concentrations and cecal extract nesfatin-1 immunoreactivity were significantly higher in the DYS group than in the CON and FMT groups (Figure 3A,B). FMT treatment significantly reduced the elevated nesfatin-1 concentrations observed after DYS, shifting values toward those of the CON group, although they remained significantly different from the CON group (Figure 3A,B). Because matrix-specific validation was not performed for cecal extracts, the cecal measurements are interpreted as assay-detected immunoreactivity rather than independently validated absolute nesfatin-1 concentrations.

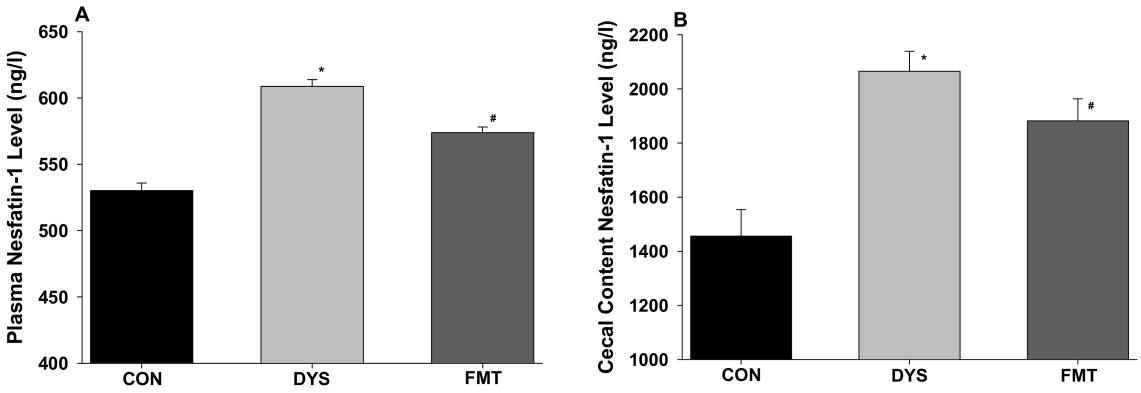


Figure 3. Nesfatin-1 immunoreactivity in plasma (**A**) and cecal contents (**B**) of rats in the CON (n = 8), DYS (n = 10), and FMT (n = 10) groups. Nesfatin-1 levels were measured by ELISA in plasma and cecal content samples collected from rats at the end of the experiment. Cecal values were obtained from cecal contents and represent assay-detected immunoreactivity; they were not normalized per gram of cecal content, were not validated for the cecal matrix, and are not directly comparable with plasma values. Values are presented as mean ± SEM. Statistical analysis was performed using one-way ANOVA followed by Tukey's post hoc test. * $p < 0.05$ indicates a significant difference between the

DYS group and the CON and FMT groups. # $p < 0.05$ indicates a significant difference between the FMT group and the CON and DYS groups.

Cecal NUCB2 mRNA expression in the pooled sample was higher in the DYS group than in the CON group and lower in the FMT group than in the DYS group (Figure 4); these data are descriptive.

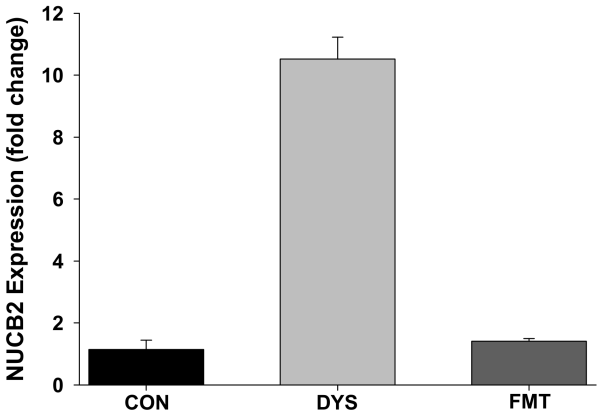


Figure 4. Cecal content NUCB2 mRNA expression in the CON, DYS, and FMT groups. Relative expression (2^−ΔΔCt, GAPDH as the internal control, CON = 1) was determined in a single pooled cecal sample per group. Bars show the mean ± SD of three technical replicates, which reflect analytical consistency and do not represent independent biological replicates. No statistical testing was performed, and the data are presented descriptively.

3.4. Effects of DYS and FMT on Histopathology and Nesfatin-1 Immunoreactivity in the Stomach

H&E staining revealed no apparent differences in the general histological architecture of the gastric fundic mucosa among the CON, DYS, and FMT groups. The overall organization of the fundic glands and the morphological characteristics of the mucosal cellular components appeared comparable across all three groups. In tangential sections through the fundic region of the stomach, distinct cell types were identified within the fundic glands. Cells with morphology consistent with oxyntic (parietal) cells were mainly distributed in the neck region of the glands, interspersed among mucous neck cells, and extended into the deeper portions of the glands. These cells were readily distinguishable from other fundic gland cell types by their spherical nuclei, relatively large size, and eosinophilic cytoplasm, which was clearly visualized with the acidic dye eosin (black arrows and dotted circles; Figure 5A,C). The muscularis mucosae, forming the basal boundary of the mucosa, was also clearly visible (arrowheads).

Cells located in the isthmus region of the fundic glands exhibited positive nesfatin-1 immunoreactivity (Figure 5B). In contrast, negative or weak nesfatin-1 immunoreactivity was observed in cells located in the neck and deeper glandular regions (Figure 5D). Panel B is a serial section corresponding to panel A (as is panel D to panel C), and the same cell groups are shown at corresponding positions.

In the CON group, cells within the neck region of the fundic glands showed intense nesfatin-1 immunostaining (Figure 6A,B). Conversely, nesfatin-1 immunoreactivity was markedly reduced in the DYS group (Figure 6C,D). In the FMT group, nesfatin-1 immunoreactivity was stronger than in the DYS group but remained weaker than in the CON group (Figure 6E,F). Semi-quantitative scores were significantly lower in the DYS group than in the CON group, whereas scores in the FMT group were significantly higher than in the DYS group but remained significantly lower than in the CON group (Table 1).

Table 1. Semi-quantitative gastric nesfatin-1 immunoreactivity scores in rats following post-weaning-induced DYS and FMT.

CON	DYS	FMT
2.66 ± 0.07	1.40 ± 0.06 *	1.81 ± 0.09 #

Nesfatin-1 immunoreactivity scores for the CON (n = 8), DYS (n = 10), and FMT (n = 10) groups are presented as mean ± SEM. Statistical evaluation was performed using the Kruskal–Wallis test followed by Dunn's multiple-comparison test. * $p < 0.05$ denotes a significant difference between the DYS group and both the CON and FMT groups, whereas # $p < 0.05$ denotes a significant difference between the FMT group and the CON and DYS groups.

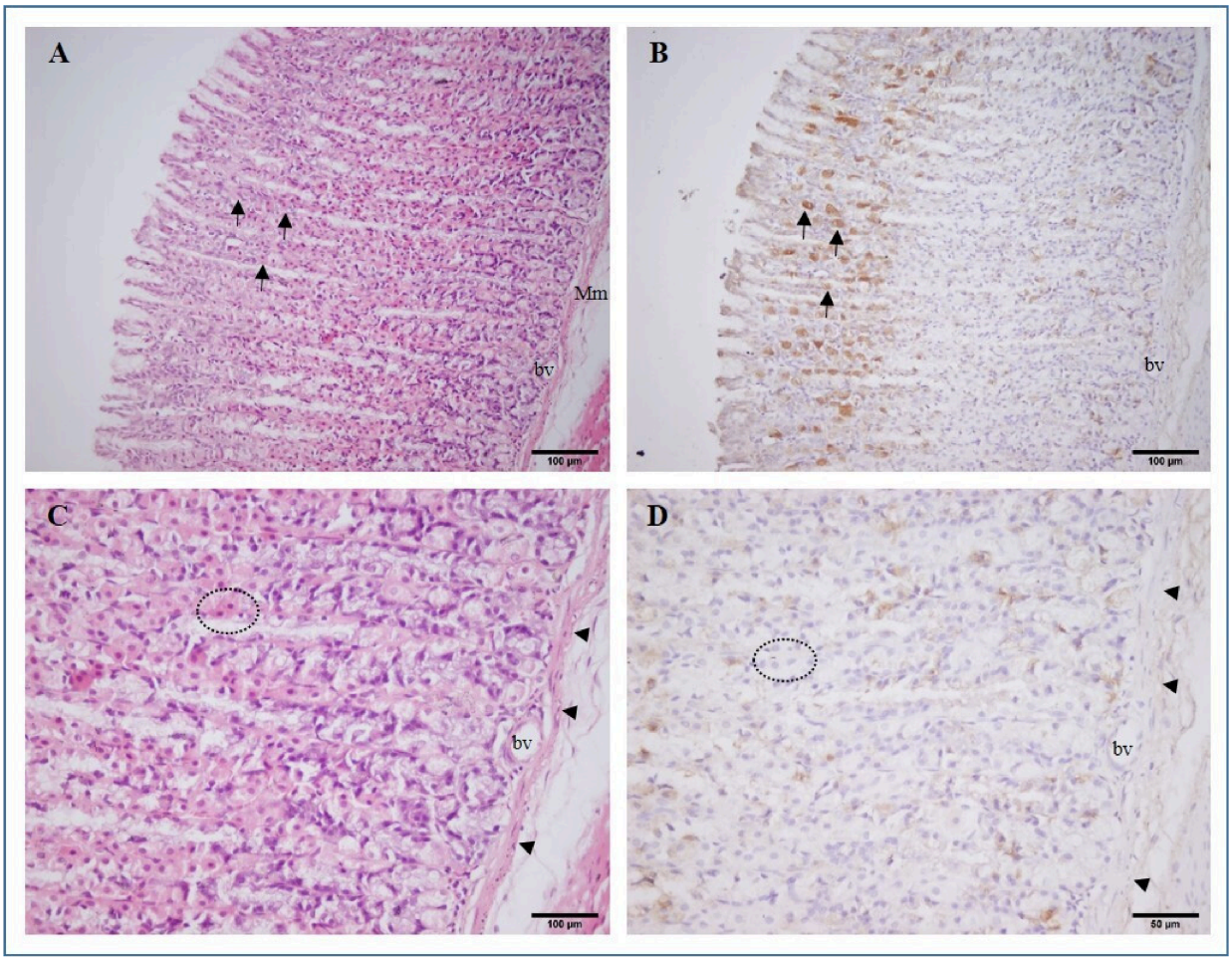


Figure 5. Histopathological examination of stomach tissue from rats in the CON, DYS, and FMT groups. Staining of a section passing tangentially through the fundus region of the stomach is shown. (**A**) H&E-stained section (×20). Arrows indicate eosinophilic cells with morphology consistent with oxyntic (parietal) cells in the gastric glands of the mucosal layer. The cytoplasm of these cells is highly eosinophilic due to its dense mitochondrial content. (**B**) Serial section of panel A immunostained for nesfatin-1 (×20); the cells indicated in panel A show nesfatin-1 immunoreactivity. (**C**) H&E-stained section (×40) showing eosinophilic cells (within the dotted circle) in the basal regions of the gland. The arrowheads indicate the muscularis mucosae of the stomach. (**D**) Serial section of panel (**C**) immunostained for nesfatin-1 (×40); the group of cells in panel (**C**) (within the dotted circle) is not immunoreactive. The black arrowheads indicate the muscularis mucosae of the stomach. Mm, muscularis mucosae; bv, blood vessel.

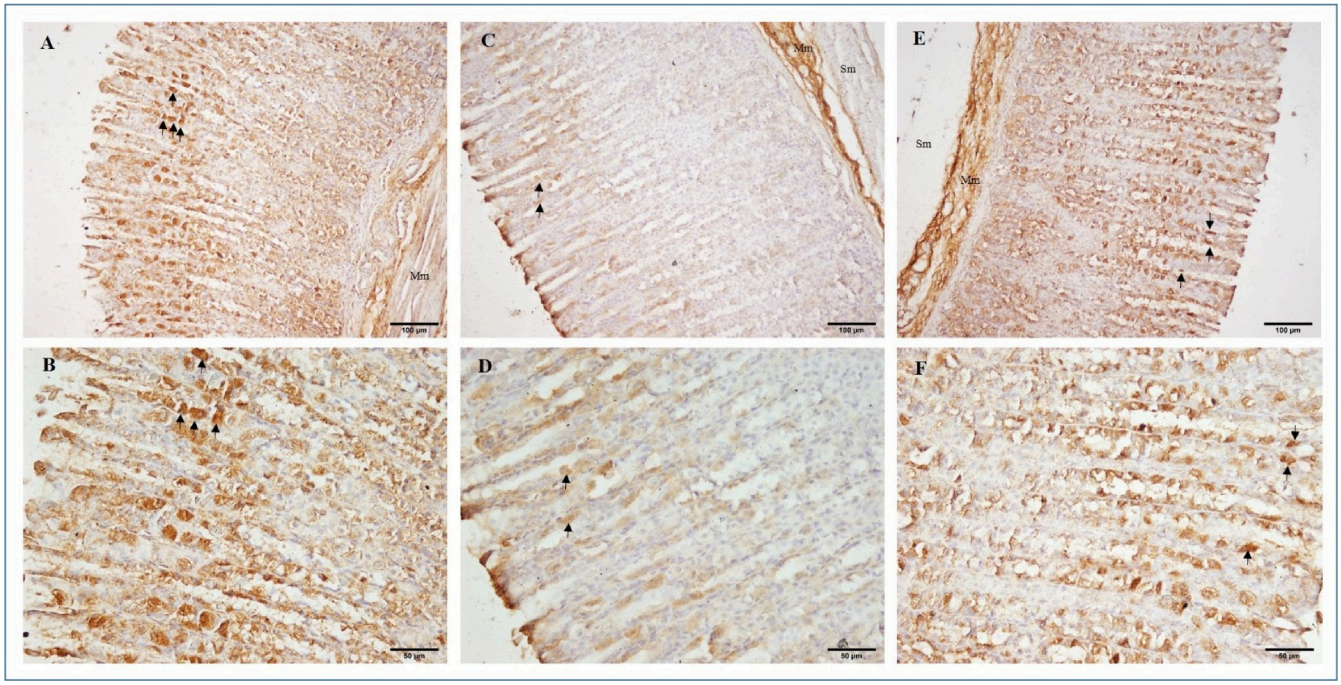


Figure 6. Immunohistochemical localization of nesfatin-1 in stomach tissue from rats in the CON, DYS, and FMT groups. Micrographs (**A**,**B**) belong to the CON group, micrographs C and D belong to the DYS group, and micrographs E and F belong to the FMT group ((**A**,**C**,**E**): ×20; (**B**,**D**,**F**): ×40). Black arrows indicate nesfatin-1-immunopositive cells localized in the gastric glands. Sm, submucosa; Mm, muscularis mucosae.

4. Discussion

The present study suggests that post-weaning DYS induced by antibiotics was associated with altered cecal microbial composition in pooled samples, reduced feed intake in cage level, and attenuated body weight gain during the growth period. DYS was also associated with alterations in the NUCB2/nesfatin-1 system, characterized by higher plasma nesfatin-1 concentrations, higher cecal nesfatin-1 immunoreactivity, higher NUCB2 mRNA expression in pooled cecal content samples, and lower gastric nesfatin-1 immunreactivity. After FMT, these alterations were partly attenuated, although values did not reach those of the CON group. Collectively, these exploratory findings are compatible with an association between post-weaning microbial perturbation and the NUCB2/nesfatin-1 system.

Diversity metrics differ in their properties, and their biological interpretation in host-associated microbiomes is not straightforward [12]; we therefore describe the detected taxa and their relative abundances rather than summarizing them with a single index. Antibiotic treatment was associated with a marked reduction in the number of detected taxa in the pooled cecal samples, consistent with previous reports that broad-spectrum antibiotics disrupt microbial community structure [9,13]. Such a loss of taxa could plausibly affect microbial fermentation products, such as short-chain fatty acids, which link diet, gut microbiota, and host energy metabolism [14]; however, these metabolites were not measured in the present study. FMT was associated with the reappearance of several taxa, a pattern consistent with FMT being used to re-establish microbial communities after disruption [3,15,16]; however, the profile was not restored to that of the control, and the dominant control taxon was not detected. Because the analysis was based on a single pooled sample per group, these observations are descriptive.

Nesfatin-1, an anorexigenic peptide derived from NUCB2, is known to participate in the regulation of food intake and of glucose and lipid metabolism [5,8]. It is expressed not only in hypothalamic neurons but also in peripheral tissues, including the gastric and in-

testinal mucosa, where it modulates gastrointestinal motility and secretion [6,17]. Potential sources of plasma nesfatin-1 include adipose tissue [18,19] and the endocrine cells of the gastric and intestinal mucosa [20–22]. The current findings are compatible with a role of the gut microbiota in modulating NUCB2/nesfatin-1 signaling. Nesfatin-1 immunoreactivity and NUCB2 mRNA were detectable in the cecal contents of all groups. These findings are consistent with an interplay between the gut microbiota and the NUCB2/nesfatin-1 system, which may represent a neuroendocrine link between intestinal health and metabolic control. In addition, DYS was associated with higher plasma nesfatin-1 concentrations, higher cecal nesfatin-1 immunoreactivity, and higher cecal NUCB2 mRNA levels, and these were lower after FMT, which is compatible with an association between the gut microbiota and the NUCB2/nesfatin-1 system. Although there is no evidence to date that the gut microbiota can regulate the NUCB2/nesfatin-1 system, nesfatin-1 has been reported to influence gut microbiota composition in neonatal bowel injury-induced DYS [23]. Nesfatin-1 immunoreactivity was detected in both plasma and cecal extracts. However, these measurements were obtained from different biological matrices, and direct quantitative comparisons between plasma and cecal extract values are not appropriate. In particular, matrix-specific validation of the cecal extracts, including dilution parallelism and spike-recovery testing, was not performed. Therefore, the cecal ELISA findings should be interpreted as assay-detected immunoreactivity rather than as independently validated absolute concentrations. Further studies using matrix-specific validation and complementary analytical methods are required to confirm the identity and quantity of nesfatin-1 in cecal samples.

Furthermore, the gut-associated NUCB2/nesfatin-1 findings of the current study suggest that gut microbiota alterations may contribute to the regulation of peripheral nesfatin-1 levels, although the precise source and underlying mechanisms remain to be determined. Immunohistochemistry showed strong nesfatin-1 immunoreactivity in the nesfatin-1-immunoreactive cells in the gastric fundic glands of CON rats, reduced staining in the DYS group, and partial recovery after FMT. The reduction in gastric nesfatin-1 immunoreactivity after DYS, together with its partial recovery after FMT, suggests that alterations in the gut microbial environment may be associated with changes in gastric nesfatin-1 signaling. However, the mechanisms underlying this association remain to be determined. It is also notable that gastric immunoreactivity decreased whereas plasma nesfatin-1 increased in the DYS group; this may reflect increased release from, or depletion of, gastric stores, altered nutritional status, or contributions from other tissues, and it cannot be resolved with the present data. In addition, the changes in nesfatin-1 immunoreactivity after DYS and FMT are consistent with a previous report showing that various factors, which may also affect the intestinal microbiota, can regulate nesfatin-1 synthesis in gastric mucosal cells [24].

Moreover, post-weaning DYS was associated with reduced feed intake and decreased body weight gain. This finding is consistent with previous reports of similar reductions in feed consumption and growth performance in developing rats treated with the same broad-spectrum antibiotics used in the present study [9]. Likewise, our results align with earlier evidence that oral antibiotic-induced DYS suppresses feed intake and body weight gain in adult rats [25,26]. In the present study, DYS was associated with reduced feed intake and attenuated body weight gain, whereas an increasing trend in feed intake was observed following FMT. These findings suggest a possible association between alterations in the gut microbial environment and feeding behavior during the post-weaning period. However, feed intake was assessed at the cage level, with only two cages per experimental group, and therefore these observations should be interpreted descriptively rather than as definitive evidence of statistically significant treatment effects. The gut microbiota may influence appetite and growth through effects on food intake regulation and energy homeostasis [27].

The reduced feed intake and body weight gain observed in DYS may therefore be related to the changes in the NUCB2/nesfatin-1 system observed here, for example if DYS activated the NUCB2/nesfatin-1 system and thereby suppressed appetite and growth. However, this explanation is speculative: nesfatin-1 was measured only at the end of the experiment, the association between nesfatin-1 and feed intake was not tested directly, and the antibiotics themselves may have reduced feed intake independently of the microbiota. Conversely, reduced feed intake may itself alter nesfatin-1 expression and release. In the present study, feed consumption was assessed at the cage level rather than individually, because the animals were group-housed to avoid the stress and behavioral alterations associated with individual housing and social isolation. Although feed intake was normalized to the number of animals per cage, only two cages were included per experimental group; the recorded values are therefore estimates of average cage-level consumption, may not reflect individual differences in feeding behavior, and cannot be separated from cage effects. Nevertheless, these measurements provide a general indication of feed consumption in each group and complementary information for interpreting the observed body weight changes.

The findings of the current study are consistent with the possibility that the gut microbial environment influences NUCB2/nesfatin-1-mediated signaling, suggesting a potential link between gut microbial integrity and host metabolic regulation. They provide a basis for exploring how microbiota-derived signals may influence neuroendocrine pathways involved in appetite control and energy balance, including the NUCB2/nesfatin-1 axis. Future research should aim to elucidate the molecular and microbial mediators underlying this interaction, such as short-chain fatty acids, microbial peptides, or bile acid metabolites, and determine whether modulation of the NUCB2/nesfatin-1 pathway through microbiota-targeted interventions could represent a therapeutic strategy for metabolic disorders associated with DYS.

An important limitation of this study is that cecal content samples were pooled within each experimental group before metagenomic analysis, resulting in a single composite sample per group. This approach provided an exploratory overview of group-level microbial composition and allowed preliminary observations regarding antibiotic-induced DYS and the potential changes associated with FMT. Similarly, NUCB2 mRNA expression was evaluated using pooled cecal content samples, which limited the assessment of individual-level variability. Nevertheless, the observed differences in plasma nesfatin-1 concentrations and cecal nesfatin-1 immunoreactivity, as determined by ELISA, provided complementary observations of differences among the experimental groups and were consistent with the observed changes in the NUCB2/nesfatin-1-related profile. However, these measurements do not overcome the limitations associated with pooled metagenomic and gene expression analyses. In particular, pooling did not permit the assessment of inter-individual variability in microbial composition or NUCB2 mRNA expression. Therefore, the metagenomic and NUCB2 mRNA findings should be interpreted as descriptive and preliminary observations. Future studies involving individual animal-level metagenomic and gene expression analyses with adequate biological replication are warranted to validate these findings and provide a more comprehensive understanding of microbiota alterations following DYS induction and FMT.

5. Conclusions

Post-weaning antibiotic-induced dysbiosis in rats was associated with reduced feed intake and body weight gain, higher plasma nesfatin-1 concentrations, higher cecal nesfatin-1 immunoreactivity and NUCB2 mRNA expression, and lower gastric nesfatin-1 immunoreactivity. After FMT, these changes showed a partial return toward control values. These exploratory findings suggest a link between the gut microbial environment and

NUCB2/nesfatin-1 signaling during the post-weaning period; however, causality, the source of cecal nesfatin-1 and NUCB2, and the underlying mechanisms need to be clarified in future studies with individual-level microbiota data and appropriate controls.

The antibiotic-induced DYS and subsequent FMT approach used in this study is based on previously established experimental protocols. The observed changes in growth, gut microbiota composition, and NUCB2/nesfatin-1-related parameters suggest a potential relationship between intestinal microbial alterations and host physiological responses. Although additional mechanisms may contribute to these effects, the present findings provide a useful basis for further investigating the interaction between gut microbiota and NUCB2/nesfatin-1-related pathways.

Supplementary Materials: The following supporting information can be downloaded at https://www.mdpi.com/article/10.3390/life16111953/s1. Table S1: Ingredient (A) and proximate nutrient (B) composition of the standard chow diet used in rats; Table S2: Relative abundance of taxa detected by shotgun metagenomic sequencing in the pooled cecal samples of the CON, DYS, and FMT groups.

Author Contributions: G.G.-B., conceptualization, methodology, investigation, formal analysis, writing—review and editing; S.F.-B., investigation and methodology; G.A., investigation and methodology; F.D., investigation and methodology; D.G.-Y., investigation and methodology; G.T., investigation and methodology; Z.S., investigation; D.U., investigation and formal analysis; M.Y., conceptualization, methodology, formal analysis, investigation, writing—original draft, writing—review and editing, funding acquisition. All authors critically revised the manuscript and approved the final version for publication. All authors have read and agreed to the published version of the manuscript.

Funding: This research was funded by Bursa Uludag University Scientific Research Project Foundation, grant number TGA-2022-1216.

Institutional Review Board Statement: All experimental procedures were approved by Bursa Uludag University Animal Experimentation Local Ethics Committee (Approval No: 2022-12/01, Approval Date: 13 September 2022).

Informed Consent Statement: Not applicable.

Data Availability Statement: Experimental data are available upon request.

Acknowledgments: The research presents a part of the findings of a Master's thesis carried out by Songul Fidan-Bulut at Bursa Uludağ University under the supervision of Murat Yalcin.

Conflicts of Interest: The authors declare that they have no competing financial or personal interests that could have influenced the work reported in this paper.

Abbreviations

The following abbreviations are used in this manuscript:

DYS	Dysbiosis
NUCB2	Nucleobindin-2
FMT	Fecal microbiota transplantation
CON	Control
H&E	Hematoxylin and Eosin

References

1. Jyoti Dey, P. Mechanisms and implications of the gut microbial modulation of intestinal metabolic processes. *npj Metab. Health Dis.* **2025**, *3*, 24. [CrossRef] [PubMed]
2. Valdes, A.M.; Walter, J.; Segal, E.; Spector, T.D. Role of the gut microbiota in nutrition and health. *BMJ* **2018**, *361*, k2179. [CrossRef] [PubMed]

3. Fan, Y.; Pedersen, O. Gut microbiota in human metabolic health and disease. *Nat. Rev. Microbiol.* **2021**, *19*, 55–71. [CrossRef] [PubMed]
4. Appleton, J. The gut-brain axis: Influence of microbiota on mood and mental health. *Integr. Med.* **2018**, *17*, 28–32.
5. Oh-I, S.; Shimizu, H.; Satoh, T.; Okada, S.; Adachi, S.; Inoue, K.; Eguchi, H.; Yamamoto, M.; Imaki, T.; Hashimoto, K.; et al. Identification of nesfatin-1 as a satiety molecule in the hypothalamus. *Nature* **2006**, *443*, 709–712. [CrossRef] [PubMed]
6. Goebel-Stengel, M.; Wang, L. Central and peripheral expression and distribution of NUCB2/nesfatin-1. *Curr. Pharm. Des.* **2013**, *19*, 6935–6940. [CrossRef] [PubMed]
7. Foo, K.S.; Brismar, H.; Broberger, C. Distribution and neuropeptide coexistence of nucleobindin-2/nesfatin-1 in the rat CNS. *Neuroscience* **2008**, *156*, 563–579. [CrossRef] [PubMed]
8. Stengel, A.; Tache, Y. Minireview: Nesfatin-1-An emerging new player in the brain-gut, endocrine, and metabolic axis. *Endocrinology* **2011**, *152*, 4033–4038. [CrossRef] [PubMed]
9. Tulstrup, M.V.; Roager, H.M.; Thaarup, I.C.; Frandsen, H.L.; Frokiaer, H.; Licht, T.R.; Bahl, M.I. Antibiotic treatment of rat dams affects bacterial colonization and causes decreased weight gain in pups. *Commun. Biol.* **2018**, *1*, 145. [CrossRef] [PubMed]
10. Paramsothy, S.; Kamm, M.A.; Kaakoush, N.O.; Walsh, A.J.; van den Bogaerde, J.; Samuel, D.; Leong, R.W.L.; Connor, S.; Ng, W.; Paramsothy, R.; et al. Multidonor intensive faecal microbiota transplantation for active ulcerative colitis: A randomized placebo-controlled trial. *Lancet* **2017**, *389*, 1218–1228. [CrossRef] [PubMed]
11. Chen, R.; Xu, Y.; Wu, P.; Zhou, H.; Lasanajak, Y.; Fang, Y.; Tang, L.; Ye, L.; Li, X.; Cai, Z.; et al. Transplantation of fecal microbiota rich in short-chain fatty acids and butyric acid treats cerebral ischemic stroke by regulating gut microbiota. *Pharmacol. Res.* **2019**, *148*, 104403. [CrossRef] [PubMed]
12. Reese, A.T.; Dunn, R.R. Drivers of microbiome biodiversity: A review of general rules, feces, and ignorance. *mBio* **2018**, *9*, e01294–e01318. [CrossRef] [PubMed]
13. Ma, N.; Tian, Y.; Wu, Y.; Ma, X. Contributions of the interaction between dietary protein and gut microbiota to intestinal health. *Curr. Protein Pept. Sci.* **2017**, *18*, 795–808. [CrossRef] [PubMed]
14. den Besten, G.; van Eunen, K.; Groen, A.K.; Venema, K.; Reijngoud, D.J.; Bakker, B.M. The role of short-chain fatty acids in the interplay between diet, gut microbiota, and host energy metabolism. *J. Lipid Res.* **2013**, *54*, 2325–2340. [CrossRef] [PubMed]
15. Contarino, M.F.; van Hilten, J.J.; Kuijper, E.J. Targeting the gut–brain axis with fecal microbiota transplantation: Considerations on a potential novel treatment for parkinson's disease. *Mov. Disord. Clin. Pract.* **2022**, *10*, S21–S25. [CrossRef] [PubMed]
16. Zou, Z.; Lei, D.; Yin, Y.; Xu, R.; Luo, H.; Chen, T.; Liu, M.; Li, X. Frequent fecal microbiota transplantation improves cognitive impairment and pathological changes in Alzheimer's disease FAD4T mice via the microbiota-gut-brain axis. *Heliyon* **2025**, *11*, e42925. [CrossRef]
17. Kras, K.; Muszynski, S.; Tomaszewska, E.; Arciszewski, M.B. Minireview: Peripheral nesfatin-1 in regulation of the gut activity-15 years since the discovery. *Animals* **2022**, *12*, 101. [CrossRef] [PubMed]
18. Ramanjaneya, M.; Chen, J.; Brown, J.E.; Tripathi, G.; Hallschmid, M.; Patel, S.; Kern, W.; Hillhouse, E.W.; Lehnert, H.; Tan, B.K.; et al. Identification of nesfatin-1 in human and murine adipose tissue: A novel depot-specific adipokine with increased levels in obesity. *Endocrinology* **2010**, *151*, 3169–3180. [CrossRef] [PubMed]
19. Tagaya, Y.; Osaki, A.; Miura, A.; Okada, S.; Ohshima, K.; Hashimoto, K.; Yamada, M.; Satoh, T.; Shimizu, H.; Mori, M. Secreted nucleobindin-2 inhibits 3T3-L1 adipocyte differentiation. *Protein Pept. Lett.* **2012**, *19*, 997–1004. [CrossRef] [PubMed]
20. Stengel, A.; Goebel, M.; Yakubov, I.; Wang, L.; Witcher, D.; Coskun, T.; Tache, Y.; Sachs, G.; Lambrecht, N.W. Identification and characterization of nesfatin-1 immunoreactivity in endocrine cell types of the rat gastric oxyntic mucosa. *Endocrinology* **2009**, *150*, 232–238. [CrossRef] [PubMed]
21. Zhang, A.Q.; Li, X.L.; Jiang, C.Y.; Lin, L.; Shi, R.H.; Chen, J.D.; Oomura, Y. Expression of nesfatin-1/NUCB2 in rodent digestive system. *World J. Gastroenterol.* **2010**, *16*, 1735. [CrossRef] [PubMed]
22. Mohan, H.; Unniappan, S. Ontogenic pattern of nucleobindin-2/nesfatin-1 expression in the gastroenteropancreatic tissues and serum of Sprague Dawley rats. *Regul. Pept.* **2012**, *175*, 61–69. [CrossRef] [PubMed]
23. Karadeniz Cerit, K.; Koyuncuoğlu, T.; Yağmur, D.; Peker Eyüboğlu, İ.; Şirvancı, S.; Akkiprik, M.; Aksu, B.; Dağlı, E.T.; Yeğen, B.Ç. Nesfatin-1 ameliorates oxidative bowel injury in rats with necrotizing enterocolitis: The role of the microbiota composition and claudin-3 expression. *J. Pediatr. Surg.* **2020**, *55*, 2797–2810. [CrossRef] [PubMed]
24. Senin, L.L.; Al-Massadi, O.; Barja-Fernandez, S.; Folgueira, C.; Castelao, C.; Tovar, S.A.; Leis, R.; Lago, F.; Baltar, J.; Baamonde, I.; et al. Regulation of NUCB2/nesfatin-1 production in rat's stomach and adipose tissue is dependent on age, testosterone levels and lactating status. *Mol. Cell. Endocrinol.* **2015**, *411*, 105–112. [CrossRef] [PubMed]
25. Tulstrup, M.V.; Christensen, E.G.; Carvalho, V.; Linninge, C.; Ahrne, S.; Hojberg, O.; Licht, T.R.; Bahl, M.I. Antibiotic treatment affects intestinal permeability and gut microbial composition in wistar rats dependent on antibiotic class. *PLoS ONE* **2015**, *10*, e0144854. [CrossRef] [PubMed]

26. Behr, C.; Sperber, S.; Jiang, X.; Strauss, V.; Kamp, H.; Walk, T.; Herold, M.; Beekmann, K.; Rietjens, I.M.C.M.; van Ravenzwaay, B. Microbiome-related metabolite changes in gut tissue, cecum content and feces of rats treated with antibiotics. *Toxicol. Appl. Pharmacol.* **2018**, *355*, 198–210. [CrossRef] [PubMed]
27. Yu, M.; Yu, B.; Chen, D. The effects of gut microbiota on appetite regulation and the underlying mechanisms. *Gut Microbes* **2024**, *16*, 2414796. [CrossRef] [PubMed]

Disclaimer/Publisher's Note: The statements, opinions and data contained in all publications are solely those of the individual author(s) and contributor(s) and not of MDPI and/or the editor(s). MDPI and/or the editor(s) disclaim responsibility for any injury to people or property resulting from any ideas, methods, instructions or products referred to in the content.